

## A Hexagonal Perovskite Intergrowth

Compound:  $\text{La}_2\text{Ca}_2\text{MnO}_7$ \*\*

Yingxia Wang, Jianhua Lin,\* Yu Du, Ruiwen Qin, Bin Han, and Chun K. Loong

Perovskite and related compounds have attracted considerable interest during the last two decades because of their extraordinary physical properties. High- $T_c$  cuprate superconductors and colossal magnetoresistance (CMR) manganese oxides are just two examples of a number of interesting materials with such perovskite-related structures.<sup>[1–4]</sup> Although diverse compositions and structure types have been identified for perovskite-related compounds, they primarily involve alternate stacking of the perovskite layers with layers of other structural types. The Ruddlesden–Popper phases  $(\text{ABO}_3)_n\text{AO}$ <sup>[5,6]</sup> are a well-known family of perovskite intergrowth compounds; in these compounds, multiple perovskite layers  $n$  octahedra thick alternate with single AO rock salt layers. The perovskite-related AO-rich intergrowth compounds  $(\text{AO})_n\text{ABO}_3$  have also been obtained in cuprate systems such as  $\text{Bi}_2\text{Sr}_2\text{CuO}_6$  and  $\text{Tl}_2\text{Sr}_2\text{CuO}_6$ .<sup>[1,5]</sup>

In the known perovskite-related intergrowth compounds, tetragonal perovskite layers (that is, the (001) plane of cubic perovskite) are most frequently observed, and hexagonal perovskite layers (that is, the (111) plane of cubic perovskite) are rare. This structural preference clearly originates from the synergistic relationship between the interfacial structures adopted by the perovskite layers and other intergrowth components. For example, both cubic perovskite and rock salt structures have identical (001) planes with the composition “AO”; therefore, the topology of the interfacial structure remains unchanged or undergoes only a small distortion when they form an intergrowth compound. In contrast, the surface of the (111) perovskite block is a close packed  $\text{AO}_3$  layer, and a hexagonal intergrowth compound can form only when the insert layer fits into this particular structural arrangement with favorable energy over the perovskite structure. One example of what can be regarded as hexagonal perovskite intergrowth compounds is the  $\text{BaNiO}_3$  type and its derivatives.  $\text{BaNiO}_3$  is a hexagonal modification of the perovskite structure in which  $\text{AO}_3$  forms a hexagonal close packing and the  $\text{NiO}_6$  octahedra share two opposite faces to form one-

dimensional chains along the  $c$  axis. The intergrowth of cubic perovskite and the  $\text{BaNiO}_3$  type with variable periodicities of the cubic and hexagonal layer results in various polytype structures.<sup>[5,7]</sup> However, these compounds are generally considered to belong to the perovskite family rather than being new intergrowth compounds. Owing to the distinctive contribution of perovskite layers to the physical properties, such as superconductivity and colossal magnetoresistance, it is of interest to search for hexagonal perovskite intergrowth compounds and to see how the physical properties are influenced by different kinds of perovskite layers.

During studies on the  $\text{Ca/La/Mn/O}$  system, we identified the new compound  $\text{La}_2\text{Ca}_2\text{MnO}_7$ . The empirical formula of this phase was established initially by a systematic synthetic study in the phase diagram. Chemical analysis indicated that the formal oxidation state of manganese in this compound is  $\text{Mn}^{\text{IV}}$ . Crystallographic studies confirmed the composition of the compound and further established that it is an intergrowth compound formed by hexagonal perovskite and “ $\text{Ca}_2\text{O}$ ” layers.<sup>[8]</sup>

The crystal structure of  $\text{La}_2\text{Ca}_2\text{MnO}_7$  is composed of nearly ideal close-packed  $[\text{LaO}_3]$  arrays, which are stacked in sequence AABBBCC along the  $c$  axis. The Mn and Ca atoms, respectively, occupy the octahedral and trigonal-prismatic sites between the closed-packed  $[\text{LaO}_3]$  sheets. Figure 1 shows the structure of  $\text{La}_2\text{Ca}_2\text{MnO}_7$ ; the Mn atoms lie within the octahedra. Scheme 1 shows the packing sequence in the structure of  $\text{La}_2\text{Ca}_2\text{MnO}_7$ .

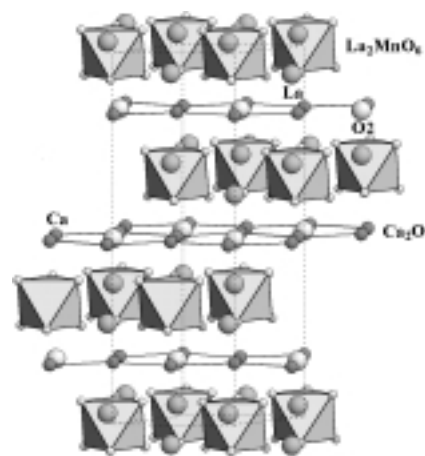
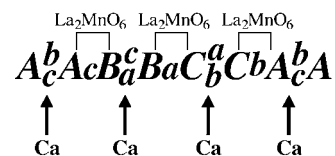


Figure 1. Crystal structure of  $\text{La}_2\text{Ca}_2\text{MnO}_7$ ; Mn atoms lie within the octahedra, the vertices of which are formed by the O1 atoms. La1 atoms are shown as isolated dark circles. The Ca1 atoms form a graphite-like network, and the O2 atoms are located at the centers of the hexagons. For clarity, the distortion of the O2 site is not shown.



Scheme 1. The packing sequence in the structure of  $\text{La}_2\text{Ca}_2\text{MnO}_7$ . The capital letters represent the close-packed  $[\text{LaO}_3]$  layers, and the small letters represent the positions of the Mn and Ca atoms. The Ca atoms are represented by two letters, because the Ca positions are divided into two groups.

[\*] Prof. J. Lin, Dr. Y. Wang, Yu. Du, R. Qin, B. Han  
State Key Laboratory for Rare Earth Materials Chemistry  
and Applications  
Department of Materials Chemistry, Peking University  
Beijing 100871 (P.R. China)  
Fax: (+86)10-6275-1708  
E-mail: jhlin@chem.pku.edu.cn

Dr. C. K. Loong  
Intense Pulsed Neutron Source Division  
Argonne National Laboratory  
Argonne, IL 60439 (USA)

[\*\*] We are thankful for financial support from the Youth Scientist  
Excellency Foundation (29625101), NSFC (29731010), and State Key  
Basic Research Program. Work performed at Argonne is supported by  
US DOE-BES under Contract No. W-31-109-ENG-38.

Supporting information for this article is available on the WWW under  
<http://www.wiley-vch.de/home/angewandte/> or from the author.

The Mn octahedra form a single hexagonal (111) perovskite layer with the composition of  $\text{La}_2\text{MnO}_6$ . The Ca atoms are located between the hexagonal perovskite blocks and form a graphite-like sheet. The coordination polyhedron of the Ca atoms is a trigonal prism formed by six oxygen atoms in the perovskite layers. The Ca layer contains an additional oxygen atom (O2); hence, the overall composition is “ $\text{Ca}_2\text{O}$ ”. Therefore,  $\text{La}_2\text{Ca}_2\text{MnO}_7$  can be considered as an intergrowth compound in which single hexagonal perovskite (111) layers ( $\text{La}_2\text{MnO}_6$ ) stack alternately with “ $\text{Ca}_2\text{O}$ ” layers and can be described as  $(\text{La}_2\text{MnO}_6)(\text{Ca}_2\text{O})$ . Only the early rare earth elements ( $\text{Ln} = \text{La}$  to  $\text{Sm}$ ) form such compounds; the others form mixed oxides at this composition.

The Ca atoms in the “ $\text{Ca}_2\text{O}$ ” layer form a graphite-like hexagonal network, in which the additional oxygen atom (O2) is located with a sixfold distortion. This distortion can be clearly seen in the difference Fourier map shown in Figure 2. The distortion of the oxygen atoms in the Ca layer can be

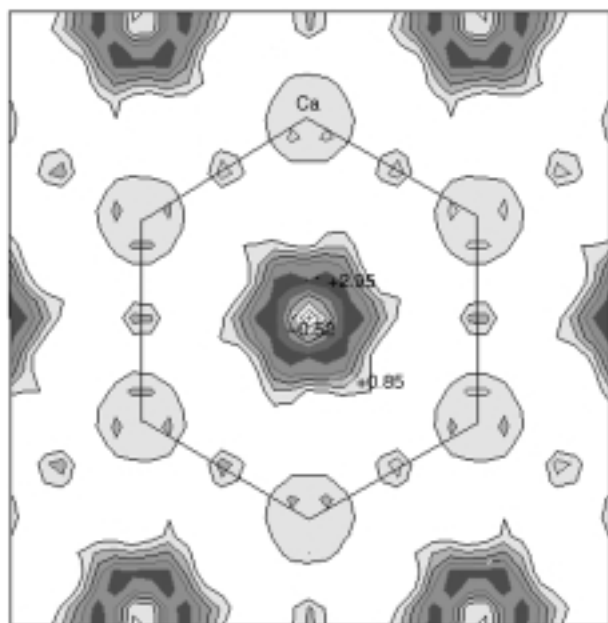


Figure 2. Electron density of the O2 position calculated from difference Fourier maps; some typical values of the electron density are shown. The Fourier map calculation was carried out by including all atoms except O2.

understood by considering their coordination environment. All of the Ca hexagonal nets are bicapped by La atoms to give hexagonal-bipyramidal polyhedra. The center of the hexagonal bipyramid is not suitable for the oxygen atom, because the distance between the opposite La atoms is too short (4.2 Å). Two other vacancies, namely, tetrahedral and triangular, are present in the hexagonal bipyramid. The triangular site is a little too small for the oxygen atoms and, from the difference Fourier map, the O2 atoms prefer to occupy the tetrahedral sites. The Ca–O2 bond length is about 2.65 Å, which is comparable with those within the trigonal prism (2.43 and 2.38 Å); therefore, the O2 atoms are capped on the rectangular faces of the Ca trigonal prisms. On average, the coordination polyhedron of the Ca atoms is a monocapped trigonal prism. In the space group  $R\bar{3}$ , the O2 atom can

approximately be represented by a general position (0.0, 0.132(2), 0.5), and the refined occupation factor is about 0.17, which agrees very well with that expected from the empirical formula (%).

In the  $\text{La}_2\text{Ca}_2\text{MnO}_7$  structure, the  $\text{MnO}_6$  octahedra are isolated; hence, we could expect rather localized physical properties for this compound.  $\text{La}_2\text{Ca}_2\text{MnO}_7$  shows Curie–Weiss paramagnetic behavior above  $-233^\circ\text{C}$  (40 K) and a weak antiferromagnetic interaction was observed at low temperature ( $\theta = 42.5$ ). The effective magnetic moment in the high-temperature range is  $\mu_{\text{eff}} = 4.0 \mu_{\text{B}}$ , which agrees with that of a spin-only isolated  $\text{Mn}^{\text{IV}}$  ion ( $3.87 \mu_{\text{B}}$ ). The conductivity of  $\text{La}_2\text{Ca}_2\text{MnO}_7$  increases from  $\sigma = 1.0 \times 10^{-4} \Omega^{-1} \text{cm}^{-1}$  at  $200^\circ\text{C}$  to about  $2.3 \times 10^{-2} \Omega^{-1} \text{cm}^{-1}$  at  $770^\circ\text{C}$ .

$\text{La}_2\text{Ca}_2\text{MnO}_7$  is a novel example of a hexagonal perovskite intergrowth compound, formed by alternative stacking of hexagonal perovskite ( $\text{La}_2\text{MnO}_6$ ) and “ $\text{Ca}_2\text{O}$ ” layers. Unlike the  $\text{BaNiO}_3$  derivatives, the building blocks in this compound are of two distinct structure types, and it therefore provides a new principle for rational synthesis of perovskite-related compounds. Comparison with the Ruddlesden–Popper phases  $(\text{ABO}_3)_n\text{AO}$  suggests the existence of the hexagonal perovskite intergrowth analogue  $(\text{La}_{n+1}\text{Mn}_n\text{O}_{3n+3})(\text{Ca}_2\text{O})$ . According to this formula,  $\text{La}_2\text{Ca}_2\text{MnO}_7$  is the  $n = 1$  member of this hexagonal perovskite intergrowth family. Accordingly, the cubic perovskite or  $\text{BaNiO}_3$ -type structure is the end-member with  $n = \infty$  in this family. The compounds of  $n > 1$  in this family should contain two-dimensional hexagonal perovskite blocks formed by corner-sharing Mn octahedra; we could therefore expect stronger magnetic interactions between the transition metal atoms, which may lead to interesting physical properties.

### Experimental Section

A stoichiometric mixture of  $\text{La}(\text{NO}_3)_3$ ,  $\text{Ca}(\text{NO}_3)_2$ , and  $\text{Mn}(\text{NO}_3)_2$ , and an excess of citric acid (1:1.2) were dissolved in water. After removing  $\text{H}_2\text{O}$ , the mixture was heated at about  $600^\circ\text{C}$  in a furnace, and a fine powder of the mixed oxides was obtained. The product  $\text{La}_2\text{Ca}_2\text{MnO}_7$  was obtained by further heating the mixed oxides at  $900^\circ\text{C}$  for 2 d. X-ray powder diffraction on a Rigaku D/Max-2000 diffractometer indicated that single-phase products can be obtained as long as a stoichiometric mixture of starting materials is used. The formal oxidation state of manganese, as determined by the oxalate titration method, is 3.99(2).

Received: February 21, 2000 [Z14743]

- [1] J. B. Goodenough, A. Manthiram in *Chemistry of High Temperature Superconductors* (Ed.: C. N. R. Rao), World Scientific, London, **1991**, p. 1.
- [2] H. Müller-Buschbaum, *Angew. Chem.* **1989**, *101*, 1503; *Angew. Chem. Int. Ed. Engl.* **1989**, *28*, 1472.
- [3] R. von Helmolt, J. Wecker, B. Holzapfel, L. Schultz, K. Sanwer, *Phys. Rev. Lett.* **1993**, *71*, 2331.
- [4] B. Raveau, A. Maignan, C. Martin, M. Hervieu, *Chem. Mater.* **1998**, *10*, 2641.
- [5] C. N. R. Rao, B. Raveau, *Transition Metal Oxides*, 2nd ed., Wiley-VCH, Weinheim, **1998**, p. 61.
- [6] P. D. Battle, W. R. Branford, A. Mihut, M. J. Rosseinsky, J. Singleton, J. Sloan, L. E. Spring, J. F. Vente, *Chem. Mater.* **1999**, *11*, 674.
- [7] G. B. Hyde, S. Andersson, *Inorganic Crystal Structures*, Wiley, New York, **1989**, p. 74.
- [8] The crystal structure of  $\text{La}_2\text{Ca}_2\text{MnO}_7$  was solved by direct methods (Sirpow92)<sup>[9]</sup> on X-ray powder diffraction data and refined by the

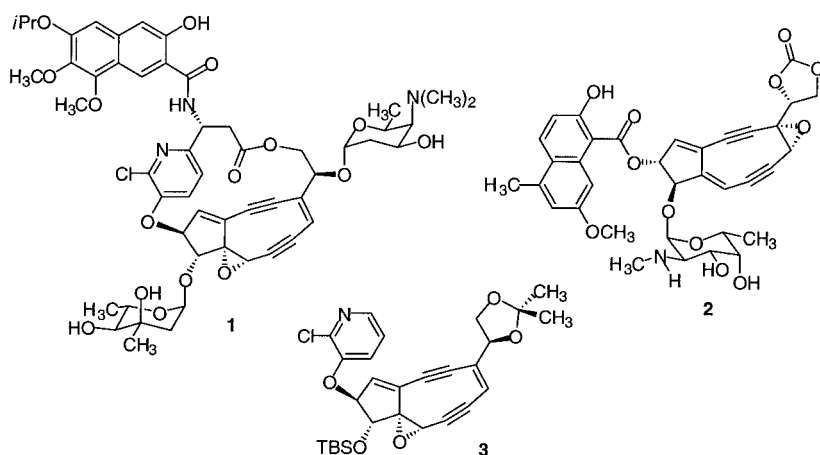
Rietveld method (GSAS)<sup>[10]</sup> on both X-ray and neutron diffraction data ( $R_p = 0.058$ ,  $R_{wp} = 0.084$ ).  $\text{La}_2\text{Ca}_2\text{MnO}_7$  crystallizes in the space group  $R\bar{3}$  (no. 148),  $Z = 3$ , with the lattice constants  $a = 5.62176(4)$ ,  $c = 17.3161(2)$ ,  $V = 473.968(7)$ . The refined atomic coordinates are Mn1: (3a) 0, 0, 0; La1: (6c) 0, 0, 0.37757(3); Ca1: (6c) 0, 0, 0.82745(7); O1: (18f) 0.0148(4), 0.502(3), 0.6024(1); O2: (18f) 0, 0.128(1), 0.5. The refined  $x$  and  $z$  values of the O2 position were  $x = -0.026(15)$  and  $z = 0.499(3)$ , which are very close to 0 and  $\frac{1}{2}$ , they were therefore fixed to improve the displacement parameters. The occupation factor of O2 was refined and fixed to  $\frac{1}{2}$  in the final refinement. The refinement also indicates mutual replacement of La and Ca atoms at the La1 and Ca1 positions, and the ratio was refined and fixed to La1: La/Ca = 0.933/0.077 and Ca1: Ca/La = 0.933/0.077 in the final refinement.

- [9] A. Altomare, M. C. Burla, M. Camalli, G. Cascarano, C. Giacovazzo, A. Guagliardi, G. Polidori, *J. Appl. Crystallogr.* **1994**, *27*, 435.  
 [10] A. C. Larson, R. B. von Dreele, Report LAUR 86-748, Los Alamos National Laboratory, **1985**.

## Synthesis of the Kedarcidin Core Structure by a Transannular Cyclization Pathway\*\*

Andrew G. Myers\* and Steven D. Goldberg

Kedarcidin is a chromoprotein enediyne antibiotic that is marked by the structural complexity and extraordinary reactivity of its chromophore component (**1**).<sup>[1]</sup> Like the related chromoprotein natural product neocarzinostatin,<sup>[1, 2]</sup> kedarcidin exhibits potent antitumor activity. The kedarcidin chromophore (**1**) and neocarzinostatin chromophore (**2**) share a common bicyclic carbon skeleton, but the site of epoxidation in the two structures is different (Scheme 1). As a

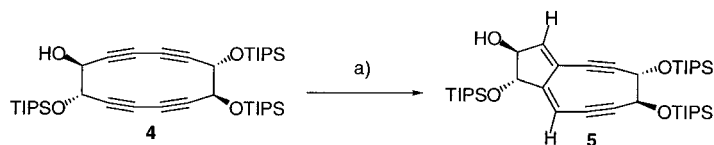


Scheme 1. The structures of kedarcidin chromophore (**1**), neocarzinostatin chromophore (**2**), and the synthetic kedarcidin core structure **3**.

[\*] Prof. A. G. Myers, S. D. Goldberg  
 Department of Chemistry and Chemical Biology  
 Harvard University  
 Cambridge, MA 02138 (USA)  
 Fax: (+1) 617-495-4976  
 E-mail: myers@chemistry.harvard.edu

[\*\*] Financial support from the National Institutes of Health is gratefully acknowledged.

result of this difference **1**, which contains a conjugated (*Z*)-enediyne group, is capable of cycloaromatization upon mild thermal activation alone (facile at 37 °C), whereas **2** requires nucleophilic activation for biradical formation.<sup>[2, 3]</sup> The reactivity of compound **1** and also its many unusual structural features—a highly unsaturated and strained core, bridging macrolactone, 2-chloro-3-pyridyl ether, and  $\beta$ -amino ester functionalities, as well as uncommon carbohydrate residues—make it an exceedingly challenging synthetic problem. Outstanding progress toward this goal has been achieved in Hirama's laboratory, including the preparation of a functional core model.<sup>[4]</sup> Recently, we described a new strategic approach to the synthesis of the common bicyclic carbon skeleton of **1** and **2** that featured the reductive transannular cyclization of a tetrayne precursor promoted by hydride addition (**4**  $\rightarrow$  **5**, Scheme 2).<sup>[5]</sup> Unresolved issues regarding the



Scheme 2. Reductive transannular cyclization of the tetrayne **4**. a) KHMDS,  $\text{NaAlH}(\text{OCH}_2\text{CH}_2\text{N}(\text{CH}_3)_2)_3$ , THF,  $-78^\circ\text{C}$ , 50–54 %.<sup>[5]</sup>

adaptation of this approach to the synthesis of the kedarcidin core structure were the compatibility of the hydride reagent with a more highly functionalized substrate that would be suitable for the synthesis of **1**, the problem of regio- and stereoselective epoxidation of the diene product, and the introduction of the central olefin of the (*Z*)-enediyne group. These problems have been addressed, as described herein, within the context of an enantioselective synthesis of the kedarcidin core structure **3** (Scheme 1).

The prior reductive cyclization (**4**  $\rightarrow$  **5**) was problematic with regard to a synthesis of **1** from two standpoints: (1) the requirement for a free propargylic hydroxyl group to direct the hydride addition meant that introduction of the pyridyl ether of **1** must occur after formation of the reactive core, and (2), as discussed, functional group compatibility was limited by the strongly reducing hydride reagent. To address these problems we considered an alternative strategy for the generation of the vinyl–metal intermediate believed to mediate the transannular ring closure, one involving low-temperature lithium–halogen exchange within a vinyl halide precursor such as the bromide **6**. To test this hypothesis, precursor **6** was synthesized, using as starting materials the dibromoolefin **7** and the diyne **8**,<sup>[6]</sup> two optically pure components of similar size and complexity (Scheme 3).

The enantioselective synthesis of the dibromoolefin **7**, a molecule with a latent  $C_2$ -symmetry axis, evolved from the exploration of several different synthetic routes, and ulti-